Inhibition of Androgen-Independent Prostate Cancer by Estrogenic Compounds Is Associated with Increased Expression of Immune-Related Genes[1]

Ilsa M. Coleman, Jeffrey A. Kiefer†,2, Lisha G. Brown†, Tiffany E. Pitts†, Peter S. Nelson*, Kristen D. Brubaker†,3, Robert L. Vessella† and Eva Corey†*

*Fred Hutchinson Cancer Research Center, Seattle, Seattle, WA, USA; †Department of Urology, Medical School, University of Washington, Seattle, WA, USA

Abstract

The clinical utility of estrogens for treating prostate cancer (CaP) was established in the 1940s by Huggins. The classic model of the anti-CaP activity of estrogens postulates an indirect mechanism involving the suppression of androgen production. However, clinical and preclinical studies have shown that estrogens exert growth-inhibitory effects on CaP under low-androgen conditions, suggesting additional modes whereby estrogens affect CaP cells and/or the microenvironment. Here we have investigated the activity of 17β estradiol (E2) against androgen-independent CaP and identified molecular alterations in tumors exposed to E2. E2 treatment inhibited the growth of all four androgen-independent CaP xenografts studied (LuCaP 35V, LuCaP 23.1AI, LuCaP 49, and LuCaP 58) in castrated male mice. The molecular basis of growth suppression was studied by cDNA microarray analysis, which indicated that multiple pathways are altered by E2 treatment. Of particular interest are changes in transcripts encoding proteins that mediate immune responses and regulate androgen receptor signaling. In conclusion, our data show that estrogens have powerful inhibitory effects on CaP *in vivo* in androgen-depleted environments and suggest novel mechanisms of estrogen-mediated antitumor activity. These results indicate that incorporating estrogens into CaP treatment protocols could enhance therapeutic efficacy even in cases of advanced disease.

Neoplasia (2006) **8,** 862–878

Keywords: Prostate cancer, estrogen, estradiol, androgen independence, interferon-regulated genes.

Introduction

Despite substantial attention, the development of androgen-independent prostate cancer (CaP) is not well understood. Progression to an androgen-independent state represents resistance to suppression of the primary signaling pathway used to control recurrent CaP. Accordingly, an evaluation of the activities and mechanisms of new therapeutics that specifically target androgen-independent CaP growth is of special therapeutic interest.

For some 30 years, estrogens, particularly diethylstilbestrol (DES), were commonly used in the initial treatment of advanced CaP [1–6]. Originally, it was believed that the responses of CaP to estrogen therapy were mediated primarily by the suppression of the hypothalamic–hypophyseal axis and the consequent reduction in testosterone levels [7–10]. However, DES treatment was associated with significant side effects, and the Veterans Administration Cooperative Urological Research Group (VACURG), in 1967, recommended that hormonal therapy with DES be withheld until symptoms of metastatic disease appeared and that administration of DES at a level of 5 mg/day was associated with an excessive risk of cardiovascular mortality [11,12]. In a further study, VACURGII compared various dosages of DES and concluded that 1 mg/day is as effective as 5 mg/day in controlling T3 M^+ CaP [13]. In 1988, however, even this level of DES was found to be associated with a high risk for cardiovascular problems, mainly in patients over 75 years of age [14]. The use of DES in the treatment of CaP ended with the advent of luteinizing hormone–releasing hormone analogs, which are now mainly used as a means of chemical castration.

Nevertheless, published studies suggest that: 1) estrogens inhibited the growth of CaP by mechanisms unrelated to androgen suppression; 2) patients treated with estrogen appeared to have survived somewhat longer than patients who had undergone surgical castration [3]; 3) administration of

Abbreviations: CaP, prostate cancer; DES, diethylstilbestrol; PSA, prostate-specific antigen; ERβ, estrogen receptor β; E2, 17β estradiol; BrdU, 5-bromo-2-deoxyuridine; *EGP*, epithelial glycoprotein; GAPDH, glyceraldehyde-3-phosphate dehydrogenase; AR, androgen receptor; IFN, interferon

Address all correspondence to: Eva Corey, PhD, Department of Urology, University of Washington, Mailstop 356510, Seattle, WA 98195, USA. E-mail: ecorey@u.washington.edu

[1]This research was supported by grants DAMD17-01-1-0114 (E.C.) and W81XWH-04-1-0198 (E.C.) from the US Army Medical Research Material Command Prostate Cancer Research Program, by grants CA97186 and CA85859 (P.S.N.) from the National Institutes of Health, and by a grant from the Signal Pharmaceutical Research Division of Celgene.

[2]Present address: Translational Genomics Research Institute (TGen), Gaithersburg, MD, USA.

[3]Present address: Department of Biological and Allied Health Sciences, Bloomsburg University, Bloomsburg, PA, USA.

Received 27 April 2006; Revised 25 July 2006; Accepted 28 July 2006.

DOI 10.1593/neo.06328

DES to patients with hormone-independent CaP suppressed prostate-specific antigen (PSA) and prolonged survival more effectively than administration of the antiandrogen flutamide [15]; and 4) Byar and Corle [4] commented that no form of endocrine therapy had been proven to be superior to 1 mg of DES daily. The hypothesis of direct inhibitory effects of estrogen on CaP is supported by observations that estrogen receptors are expressed in normal and neoplastic prostate epithelia [16–18], by observations that estrogens exhibit direct cytotoxic effects on CaP cells *in vitro* [19–23], and by our own demonstration of growth inhibition of CaP by 17β estradiol (E2) in the androgen-free environment of ovariectomized female mice [24].

The discovery of a second estrogen receptor, estrogen receptor β (ERβ), renewed interest in basic research involving estrogen pathways. Several reports have shown that ERβ is present in normal prostate epithelial cells as well as in CaP, and levels of ERβ messages and/or proteins appear to be downregulated during disease progression [16–18,25]. A straightforward hypothesis holds that ERβ transduces a growth-inhibitory effect of estrogen on CaP cells. In support of this hypothesis, a lower rate of cancer-related deaths was observed in CaP patients with ERβ *versus* CaP patients without ERβ [26], and an estrogenic compound operating through the ERβ receptor suppressed the growth of DU145 CaP cells [22,23]. In contrast to decreasing levels of ERβ with CaP progression, we have recently demonstrated that ERβ is expressed in a majority of CaP bone and soft-tissue metastases [27], as in another report on ERβ expression in a small number of CaP metastases [16]. Together, these studies suggest that estrogen action against prostate carcinoma could involve ERβ or potentially other direct modes of action such that CaP growth may be restrained even in an androgen-independent state.

The current study was undertaken to determine whether estrogenic compounds can inhibit the growth of androgen-independent CaP and to investigate phenotypic changes associated with antitumor effects. Using human CaP xenografts, our results show that estrogenic compounds clearly suppress androgen-independent growth of CaP in casthe trated hosts, calling into question the traditional view that estrogen's activity against CaP depends solely on androgen suppression. The results indicate that estrogens may be especially useful in the treatment of androgen-independent CaP. We identified several novel molecular alterations resulting from tumor exposure to E2 that may contribute to E2-mediated tumor inhibition. Further studies are warranted to exploit the antitumor effects of E2 treatment in the context of advanced CaP.

Materials and Methods

Animal Studies

Xenografts Androgen-sensitive PSA-producing CaP xenografts LuCaP 35 [28], LuCaP 23.1 [29,30], and LuCaP 58 [31] (which all originated from lymph node metastases), and androgen-insensitive neuroendocrine-type CaP xenograft LuCaP 49 (which originated from omental fat metastasis) [32] were used. The xenografts were maintained and propagated in Balb/c nu/nu intact male mice. The androgen-independent variants of LuCaP 35V and LuCaP 23.1 were developed from parental tumors on regrowth after castration [28,31] and were maintained and propagated in castrated B17 Fox Chase SCID male mice (Charles River, Wilmington, MA).

Effects of E2 on recurrent LuCaP 35 after castration All animal procedures were performed in compliance with the University of Washington Institutional Animal Care and Use Committee and National Institutes of Health guidelines. In our first study, LuCaP 35 tissue bits were implanted subcutaneously into SCID male mice. Tumor growth was monitored by measuring tumor volume twice a week. Serum was collected weekly for PSA determination. Animals were castrated when the tumors reached 200 to 400 mm^3. Animals with recurrent tumors (determined as two rising serum PSA values) were randomized into three groups of 10 animals each. Group 1 animals received placebo pellets.

Group 2 animals were supplemented with E2 by the subcutaneous implantation of slow-release Trocar pellets (90-day-release E2, 100–125 pg/ml; Innovative Research of America, Sarasota, FL), and group 3 animals were supplemented with DES pellets by the subcutaneous implantation of slow-release Trocar pellets (90-day-release DES, 0.01 mg; Innovative Research of America). Animals were sacrificed when tumors exceeded 1000 mm^3 at 90 days postimplantation or when the animals became compromised. Student's unpaired two-tailed *t*-test was used to analyze the differences between groups.

Effects of E2 on LuCaP 35V in castrated male mice In additional experiments performed to determine the effects of E2 on proliferation and gene expression, we used the androgen–independent xenograft LuCaP 35V [28]. SCID male mice were castrated at 8 weeks of age and implanted with LuCaP 35V tumor bits at least 2 weeks after surgery. Tumor growth was monitored by tumor measurements twice a week using calipers, and tumor volume was calculated as 0.5236*LHW*. Blood samples were collected weekly for the determination of serum PSA levels (IMx Total PSA Assay; Abbott Laboratories, Abbott Park, IL). When tumors reached 200 to 400 mm^3, the animals were randomized into two groups. Group 1 was supplemented with E2 by the subcutaneous implantation of slow-release Trocar pellets (60-day release, 0.05 mg; Innovative Research of America). Group 2, which received placebo pellets, was the control group. Five animals from each group were sacrificed on days 1, 3, and 7 postimplantation of E2 pellets. One hour before sacrifice, the animals were injected intraperitoneally with 80 mg/kg body weight 5-bromo-2-deoxyuridine (BrdU; Sigma-Aldrich Co., St. Louis, MO) for evaluation of tumor cell proliferation. Tumors were fixed in formalin and embedded in paraffin. The 10 remaining animals in each group were monitored for long-term assessment of tumor growth and PSA production after E2 treatment. Animals

were sacrificed when tumors exceeded 1000 mm^3 at 60 days postimplantation or when the animals became compromised. Tumors were frozen in liquid nitrogen and stored at −80°C and/or fixed with formalin and embedded in paraffin, and serum was collected for determination of E2 levels (IMx Estradiol Immunoassay; Abbott Laboratories). Student's unpaired two-tailed *t*-test was used to analyze the differences between groups, and a log-rank test was used to evaluate differences in survival.

Effects of E2 on the growth of LuCaP 23.1AI, LuCaP 49, and LuCaP 58 in castrated male mice To investigate whether the E2 inhibition of androgen-independent growth occurs with other CaP cells (not just LuCaP 35 lines), we set up similar experiments with three additional xenografts: LuCaP 35AI, LuCaP 49, and LuCaP 58. The experimental design was the same as for the study with LuCaP 35V. Tumor bits were implanted in castrated male mice (aiming for $n = 10$ per group) at least 2 weeks after surgery, and tumor growth and PSA levels were monitored. Animals bearing each particular xenograft were randomized into two groups (tumors 200–400 mm^3). Group 1 was supplemented with E2 by the subcutaneous implantation of slow-release Trocar pellets (60-day release, 0.05 mg; Innovative Research of America). Group 2, which received placebo pellets, was the control group. Animals were sacrificed when tumors exceeded 1000 mm^3 at 60 days postimplantation or when the animals became compromised. Tumors were frozen in liquid nitrogen and stored at −80°C and/or fixed with formalin and embedded in paraffin. Student's unpaired two-tailed *t*-test was used to analyze differences between groups.

Proliferation and Apoptosis Assays

Samples of LuCaP 35V tumors treated with E2 for 1, 3, and 7 days, and control tumors were fixed in formalin and embedded in paraffin. An anti-BrdU immunohistochemistry kit was used to assess the number of proliferating cells (Zymed, San Francisco, CA). Five-micrometer sections of paraffin-embedded tissues were used for the analysis, as recommended by the manufacturer. Apoptosis in tumors was assessed with a FragEL DNA fragmentation detection kit from Oncogene (La Jolla, CA), as recommended by the manufacturer. Positive nuclei or apoptotic cells were counted in five representative fields containing ~1000 cells in three samples of treated and untreated tumors from each time point. Statistical analysis was performed using Student's *t* test.

Cell Culture

Seven hundred to 900 mm^3 of LuCaP 35V tumors grown and passaged in castrated SCID mice were harvested for the isolation of epithelial cells [28]. Isolated cells were rinsed thrice and plated overnight in 10% charcoal-stripped fetal bovine serum (Hyclone, Logan, UT) in phenol red-free RPMI 1640 (Invitrogen, Carlsbad, CA). LuCaP 35V cells were treated with 10^{-8} M E2 or vehicle (0.01% EtOH) for 4 hours.

Western Blot Analysis

Following treatment with E2 or vehicle, nuclear and cytoplasmic fractions were prepared as previously published [33]. Proteins (25 μg/well) were separated by 12.5% sodium dodecyl sulfate–polyacrylamide gel electrophoresis and transferred to polyvinylidene difluoride membrane (PVDF) membranes. Blots were blocked in a 1:1 solution of NaP-Sure blocker (Geno Technology, Inc., St. Louis, MO) and Tris-buffered saline + 0.1% Tween-20 for 2 hours, then probed with a rabbit polyclonal antibody against ERβ (Affinity BioReagents, Golden, CO) for 1 hour at room temperature. ERβ immunoreactivity was detected using a goat anti–rabbit secondary antibody conjugated with horseradish peroxidase (1:2000; Amersham, Piscataway, NJ). Blots were developed using the Amersham ECL.

Electrophoretic Mobility Shift Assay (EMSA)

Nuclear extracts from LuCaP 35V treated with 10^{-8} M E2 or vehicle (0.01% EtOH) for 4 hours (25 μg) were incubated with 50 fmol of dsDNA probes for 30 minutes at 37°C in a buffer containing: 20 mM Tris (pH 8), 10 mM NaCl, 3 mM EDTA, 0.05% Nonidet P-40, 2 mM DTT, 4% glycerol, 1 mM $MgCl_2$, and 1 μg of poly dI–dC (Amersham). The binding consensus sequences used were an estrogen response element (ERE; GGATCTAGGTCACTGTGACCCCGGATC) and a mutated form of ERE (GGATCTAG*TA*CACTGTGACCCCGGATC; Santa Cruz Biotechnology, Inc., Santa Cruz, CA). Double-stranded DNA were end-labeled with [γ-^{32}P]ATP (Amersham) using T4 polynucleotide kinase (Promega, Madison, WI). For competition studies, 50 fmol of unlabeled probe was added to the reaction. Protein–DNA complexes were separated in 4% nondenaturing polyacrylamide gels.

RNA Isolation

Tumors from animals treated with E2 for 60 days and control tumors were homogenized using an Omni TH homogenizer (Omni International, Warrenton, VA), and RNA was extracted using TriPure Isolation Reagent (Roche, Indianapolis, IN), according to the manufacturer's instructions. RNA quantity was determined based on A_{260}, and the integrity of RNA was confirmed by agarose gel.

cDNA Array Analysis

PEDB cDNA microarrays containing ~7000 human prostate–derived cDNA clones were prepared on poly-L-lysine–coated glass microscope slides using a robotic spotting tool, as previously described [34–36]. Equal amounts of total RNA from five tumors of LuCaP 35V (control) and E2-treated LuCaP 35V (treatment) were pooled, and cDNA array experiments and analysis were performed as previously described [37]. For individual experiments, every cDNA was represented twice on each slide, and the experiments were performed in triplicate with a switch in fluorescent labels to account for dye effects, producing six data points per cDNA clone per hybridization probe. Data were filtered to exclude poor-quality spots, were normalized, and included clones whose expression was measurable in at least two of three arrays, reducing the initial list of 6720 clones to 5163 clones.

Gene Expression Analysis

To compare the overall expression patterns of replicate LuCaP 35V (control) and E2-treated LuCaP 35V (treatment) arrays, $\log_2$ ratio measurements were analyzed using the SAM procedure [38] (http://www-stat.stanford.edu/_tibs/SAM/). A one-sample *t*-test was used to determine whether the mean gene expression of E2-treated LuCaP 35V *versus* LuCaP 35V (control) differed significantly from zero. A false discovery rate (FDR) of < 1% was considered significant. Clones differentially expressed with an FDR < 1% were stratified based on fold change, and we chose to further evaluate only those with an average $\log_2$ (E2-treated/control) > 0.58 or < −0.58, corresponding to a differential expression effect of 1.5-fold or greater. We assigned differentially expressed genes to the following functional categories based on their annotations in the Gene Ontology database [39]: metabolism, immune/inflammatory response, proliferation/differentiation/apoptosis, signal transduction, structure/adhesion/motility, transcription regulation, translation protein synthesis, transport, or other/unknown.

To determine whether phenotypic changes observed in E2-treated tumors were enriched for genes in certain pathways, cDNA array results were subjected to Gene Set Enrichment Analysis (GSEA) [40]. For this analysis, interferon (IFN)–regulated, androgen-regulated, and estrogen-regulated gene sets were tested against our data. IFN-regulated and estrogen-regulated gene sets were generated from SuperArray Bioscience Corporation GEArray pathway-focused gene lists (http://www.superarray.com), and the androgen-regulated gene set was generated based on the results of DePrimo et al. [41]. To assess the statistical significance of the enrichment score observed in the data set for the three gene sets, we used permutation testing of phenotype labels (e.g., E2-treated *versus* controls), generating a nominal (NOM) *P* value. An FDR statistic was computed to adjust for gene set size and multiple hypothesis testing, with an FDR of < 25% considered significant.

Quantitative reverse transcription–polymerase chain reaction (qRT-PCR) First-strand cDNA synthesis was performed with 1.0 μg of pooled RNA from five animals of the E2 and control groups using oligo-dT_{18} primers according to the manufacturer's instructions (Clontech, Palo Alto, CA). Real-time PCR was carried out on cDNA samples using Platinum Quantitative PCR SuperMix-UDG reagent (Invitrogen) and performed on a Rotor-Gene 2000 (Corbett Research, New South Wales, Australia). PCR primers were designed to span an intron–exon boundary and to avoid amplification of any known pseudogene. Primers for the messages evaluated are listed in Table 1. Two microliters of cDNA was used per reaction with 200 nM primers, 0.5× Syber Green 1 (Molecular Probes, Eugene, OR), and 5.5 mM $MgCl_2$. The PCR reaction parameters were as follows: 50°C for 2 minutes and 95°C for 2 minutes (one cycle), followed by 35 cycles at 95°C for 10 seconds and annealing/extension at either 65°C or 69°C for 30 seconds;

Table 1. Primer Sequences.

Abbreviation	Name	Primer Sequence	Position		Annealing Temperature (°C)	Size (bp)	Accession Number
GAPDH	Glyceraldehyde dehydrogenase	5′ TGC ACC ACC AAC TGC TTA GC	556	575	65	86	NM_002046
		3′ GGC ATG GAC TGT GGT CAT GAG	642	622			
EGP	Epithelial glycoprotein	5′ GCT GGA ATT GTT GTG CTG GTT ATT TC	1019	1044	65	152	NM_002354
		3′ TGT GTC CAT TTG CTA TTT CCC TTC TTC	1171	1145			
CD74	CD74 antigen (invariant polypeptide, MHC class II antigen–associated)	5′ GTG CGA CGA GAA CGG CAA CTA TC	704	726	69	218	NM_001025159
		3′ GAA GAC CGC CTC TGC TGC TCT C	901	922			
HLA II DRA	MHC class II DR α	5′ CCC AGA GAC TAC AGA GAA CGT GG	714	736	69	265	NM_019111
		3′ GGG CTG GAA AAT GCT GAA GAT GAC	979	956			
HLA 1F	MHC class I F	5′ GTT GCC CAC CAC CCC ATC TCT G	628	649	65	371	NM_018950
		3′ GCT CTT CTT CCT CCA CAT CAC AG	977	999			
IFITM1	IFN-induced transmembrane protein 3 (1–8 U)	5′ CGT CGC CAA CCA TCT TCC TGT C	530	509	69	246	NM_003641
		3′ TTC ACT CAA CAC TTC CTT CCC CAA	284	307			
HLA DQB1	MHC class II DQ β_1	5′ GCC TTA TCA TCC ATC ACA GGA GTC	797	820	65	223	NM_002123
		3′ GTC ACA GCC ATC CGC CTC AAG G	999	1020			
IFITM3	IFN-induced transmembrane protein 3 (1–8 U)	5′ GTC CAA ACC TTC TTC TCT CCT GTC	250	273	69	264	NM_021034
		3′ CGT CGC CAA CCA TCT TCC TGT C	514	493			
BST2	Bone marrow stromal cell antigen 2	5′ GAG GTG GAG CGA CTG AGA AGA GA	406	428	69	204	NM_004335
		3′ GTT CAA GCG AAA AGC CGA GCA GG	610	588			
β2M	β_2-Microglobulin	5′ GAG TAT GCC TGC CGT GTG AAC CA	349	371	69	313	NM_004048
		3′ ACC TCT AAG TTG CCA GCC CTC CT	640	662			
CD59	CD59 antigen p18–20	5′ CTG CTG CTC GTC CTG GCT GTC T	149	170	69	370	NM_000611
		3′ GCT CTC CTG GTG TTG ACT TAG GG	497	519			
IFIT1	IFN-induced protein with tetratricopeptide repeat 1	5′ CTG AAA ATC CAC AAG ACA GAA TAG C	5	29	69	377	NM_001001887
		3′ GTC ACC AGA CTC CTC ACA TTT GCT	359	382			
IRF1	IFN-regulatory factor 1	5′ GTA CCG GAT GCT TCC ACC TCT CAC C	524	545	69	105	NM_002198
		3′ GCT GGA ATC CCC ACA TGA CTT CCT C	605	629			
IFI27	IFNα-inducible protein 27	5′ GTT GTG ATT GGA GGA GTT GTG G	226	247	65	193	NM_005532
		3′ GAG AGT CCA GTT GCT CCC AGT	399	419			
ERβ	Estrogen receptor β	5′ GCT AAC CTC CTG ATG CTC CTG TCC	1784	1807	65	204	NM_001437
		3′ AGC CCT CTT TGC TTT TAC TGT CCT CT	1988	1963			

the final extension was 72°C for 7 minutes. PCR reaction products were confirmed by agarose gel electrophoresis. Standard curves for each amplicon were generated from a four-fold dilution series of LNCaP cDNA run in duplicate (all standard curves had $r > 0.99$). Reactions were carried out in duplicate, and expression levels were calculated from a standard curve.

Normalization strategy The normalization scheme applied to real-time PCR results was based on the method of Vandesompele et al. [42]. This method employs multiple internal control genes to identify the most stably expressed control genes in samples of interest. The following messages were evaluated for use as internal controls: epithelial glycoprotein (EGP), glyceraldehyde-3-phosphate dehydrogenase (GAPDH), hydroxymethylbilane synthase (HMBS), hypoxanthine phosphoribosyltransferase 1 (HPRT1), and proteasome (prosome, macropain) subunit, β type, 6 (PSMB6). Real-time PCR on pooled samples was performed in duplicate, and expression levels were calculated based on standard curves, as above. The average expression levels were imported into the geNorm program (http://allserv.rug.ac.be/~jvdesomp/genorm/) to determine the two most stably expressed internal control genes. Briefly, geNorm determines the gene stability measure *M* as the average pairwise variation between a particular internal control gene and all other control genes. The stepwise exclusion of endogenous control genes with the highest *M* values resulted in the selection of GAPDH and EGP as the most stably expressed control genes. The normalization of the real-time PCR data of the gene of interest was accomplished by dividing raw expression levels by the geometric mean of the most stable endogenous control.

Results

Inhibition of Androgen-Independent CaP by E2 and DES

LuCaP 35 is an androgen-sensitive CaP xenograft, expressing PSA and wild-type androgen receptors (ARs), which recapitulates a response to androgen ablation and the development of androgen-independent CaP similar to that observed in humans [28]. Its growth in intact female mice is suppressed in comparison to that in ovariectomized female mice [24]. Therefore, we have chosen this xenograft for initial evaluation of the effects of estrogenic compounds in male mice. Surgical castration of intact male mice bearing LuCaP 35 CaP xenografts resulted in a reproducible time-dependent reduction in tumor volume and PSA serum levels. Recapitulating human disease, 88% of the tumors eventually recurred in the androgen-depleted environment, with a range in time to recurrence of 32 to 91 days (median = 61.5 days; Figure 1, *A* and *B*). Tumor recurrence was defined as two consecutive rising values of serum PSA. Without treatment, these androgen-independent tumors continued to grow and reached a size of ~1000 mm^3 by days 24 to 31 post-castration. Administration of E2 or DES inhibited the growth of recurrent LuCaP 35 tumors; at 104 days after castration, the tumor volumes were 134.3 ± 16.4 mm^3 (mean ± SEM) for

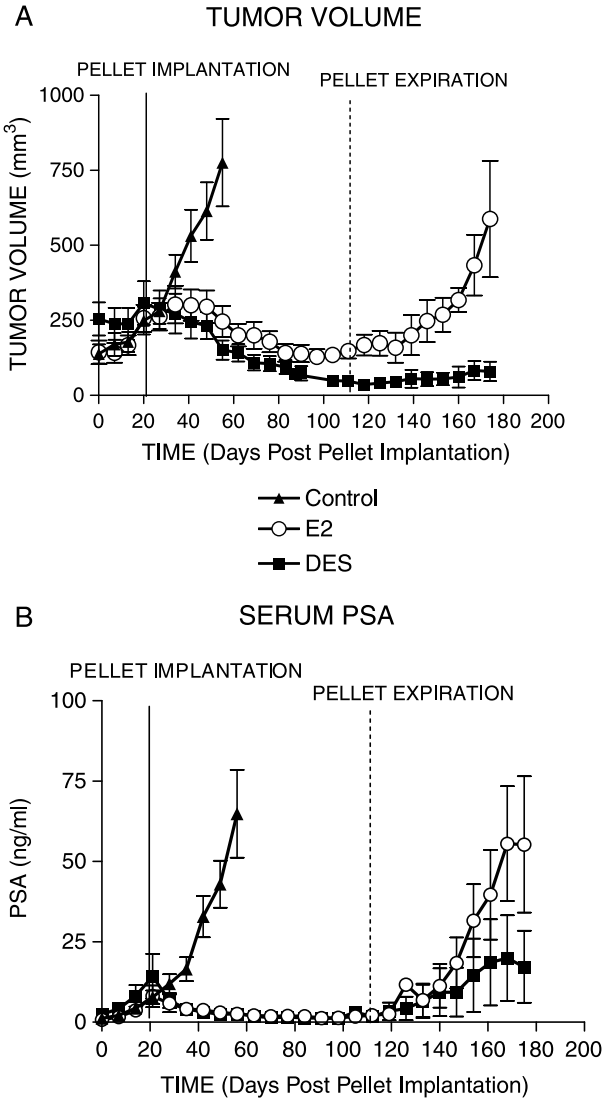

Figure 1. *Effects of estradiol on the recurrent growth of LuCaP 35 CaP xenografts. LuCaP 35 tumor bits were implanted in intact animals, and animals were castrated when tumors reached ~ 200 to 400 mm^3. Tumor volume was measured twice a week. Blood was drawn weekly for the determination of PSA serum levels. On the development of recurrent CaP, as determined by two subsequently increased PSA serum levels, animals were randomized into three groups. E2 and DES pellets were implanted in treatment animals; control animals received placebo pellets. Animals were sacrificed after tumors had reached 1000 mg or 90 days postimplantation of the pellets. Three tumors from E2-treated and DES-treated animals were monitored for an additional 670 days after pellet expiration. Data were synchronized with pellet implantation, and results are presented as mean ± SEM. (A) Tumor volume. (B) Serum PSA levels.*

E2 (with PSA levels of 1.82 ± 0.66 ng/ml) and 49.8 ± 12.1 mm^3 for DES (with PSA levels of 3.20 ± 1.86 ng/ml). Tumor volumes and PSA levels decreased, and none of the tumors reached an estrogen-resistant state during the course of the study (90 days of treatment). PSA values closely followed tumor volume. Three animals from the E2-treated and DES-treated groups were monitored for an additional 60 days after expiration of the estrogen pellets. Tumor volumes and PSA serum levels in these animals started to increase during this period (Figure 1). The tumors in animals that were treated with E2 reached 587.6 ± 194.0 mm^3 ($P = .0008$ from 90 days

after pellet expiration), with concordant rises in PSA serum levels to 55.33 ± 21.18 (P = .003; to the levels when pellets expired). Tumors in DES-treated animals started to increase in volume more slowly than E2-treated tumors after pellet expiration; the tumor volumes increased 1.5-fold (79.43 ± 32.5 mm^3) but did not reach significance (P = .3075), and PSA serum levels began to rise (17.23 ± 11.20 ng/ml; P = .0533). As observed in our previous study in female mice, administration of E2 inhibited the growth of androgen-independent LuCaP 35V xenografts in castrated male mice as well. The tumor volume of LuCaP 35V–bearing animals treated with E2 increased minimally over the original volume during the 60-day treatment period (Figure 2*A*). However, the tumor size of LuCaP 35V in the control group increased from the time of enrollment up to the time of sacrifice (days 25–35; tumor volume = 1000 mm^3; Figure 2*A*) (on day 32, P < .0001). PSA serum levels closely paralleled tumor volumes (on day 28, P = .0021) (Figure 2*B*). Levels of E2 in the control group of castrated animals with LuCaP 35V (untreated) were below the limit of assay detection (< 25 pg/ml). The level of E2 at the time of sacrifice (60 days postimplantation of E2 pellets) was 127.1 ± 22.5 pg/ml in treated LuCaP 35V animals. Survival analysis, using tumor size (≥ 1000 mm^3) as a death criterion, showed that E2 dramatically prolonged the survival of LuCaP 35V–bearing animals, as determined by log-rank test (P < .0001; Figure 2*C*).

Generalized Growth-Inhibitory Effects of E2 on Androgen-Insensitive CaP

The growth of the three additional CaP xenografts LuCaP 23.1AI, LuCaP 49, and LuCaP 58 in an androgen-free environment was inhibited by E2 administration to varying degrees (Figure 3). The tumor volume of LuCaP 23.1AI treated with E2 decreased, with significant differences from untreated tumors after 7 days of treatment (P = .00089), resulting in the near-disappearance of the tumors by day 35. PSA serum levels closely followed the tumor volume. LuCaP 58 growth was also inhibited by E2 treatment, but to a lesser extent; the tumor volume increased minimally over the original volume during the 60-day treatment period (Figure 2*A*), reaching significant inhibition *versus* untreated tumors on day 7 (P = .0137). LuCaP 49, a neuroendocrine CaP xenograft in which ARs are absent, was also inhibited by E2 administration, but the pattern of inhibition was different from those of the other three xenografts. No significant inhibition was observed for the first 10 days of treatment, after

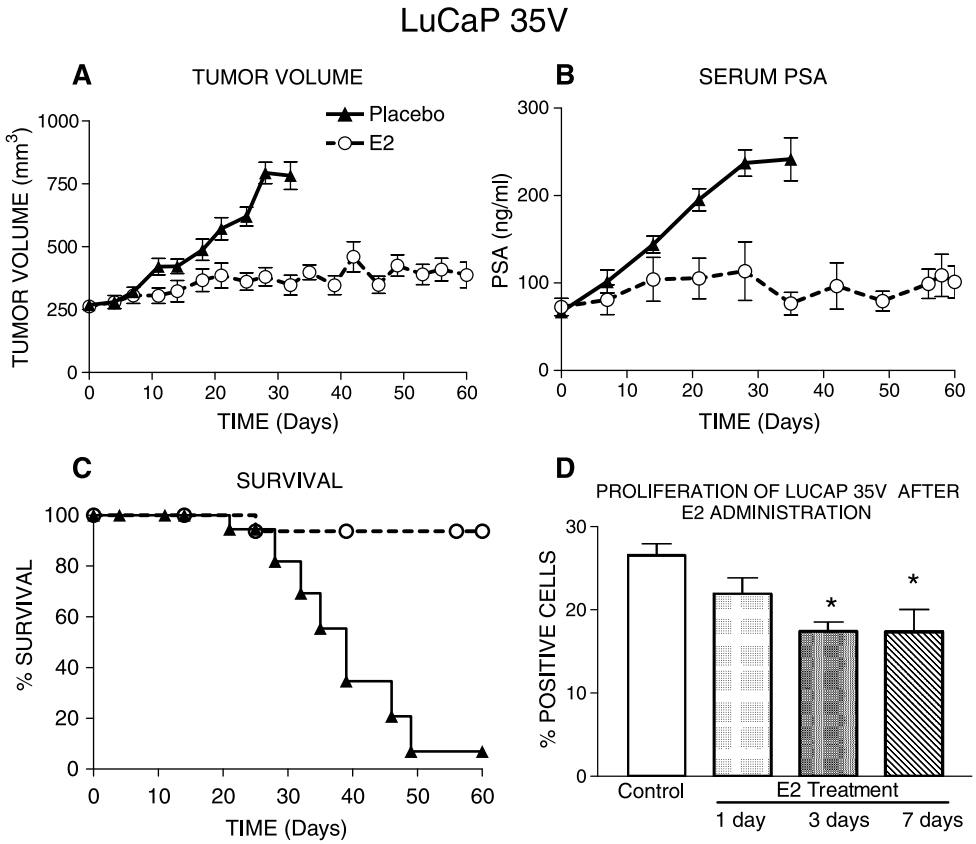

Figure 2. *Effects of estradiol on LuCaP 35V. LuCaP 35V, an androgen-insensitive CaP xenograft, was grown in castrated male SCID mice. When tumors reached 200 to 400 mm^3, animals were supplemented with 60-day-release E2 pellets, as described in Materials and Methods section. Data are presented as mean ± SEM. E2 inhibited the growth of androgen-independent LuCaP 35V in castrated male mice and caused significant increases in the survival of treated animals. PSA levels closely followed the tumor volume. (A) Tumor volume. (B) Serum PSA levels. (C) Survival. (D) Proliferation. E2 treatment decreased the proliferation of LuCaP 35V on days 3 and 7 of treatment. LuCaP 35V grown in castrated male mice was treated with E2 for 1, 3, or 7 days. BrdU staining was used to detect proliferating cells. The percentage of positive nuclei was calculated based on the counts of stained nuclei in five representative fields containing ~ 1000 cells from three samples of treated and untreated tumors from each time point. Data are presented as mean ± SEM. Statistical analysis was performed using Student's t test.*

which significant inhibition was reached (14 days, $P = .0289$). E2-treated LuCaP 49 tumors continued growing, but at a rate slower than that of untreated tumors.

Effects of E2 on Tumor Cell Proliferation and Apoptosis

To evaluate the mechanisms mediating LuCaP 35V tumor reduction after E2 treatment, we measured the incorporation of BrdU in untreated LuCaP 35V tumors *versus* tumors from mice that received E2 for 1, 3, and 7 days. The number of proliferating tumor cells decreased to 82.7 ± 7.3% of untreated tumors after 1 day (mean ± SEM), to 65.7 ± 4.2% ($P = .0063$) after 3 days, and to 65.4 ± 10.1% ($P = .0105$) after 7 days of E2 treatment (Figure 3). The rate of apoptosis in E2-treated and untreated tumors, as measured by the terminal deoxynucleotidyl transferase (TdT) FragEL DNA fragmentation detection, was not significantly different (data not shown).

Determination of E2-Mediated Alterations in Tumor Gene Expression by Microarray Analysis

Comparative analyses of cDNA microarray gene expression profiles derived from LuCaP 35V xenografts treated with E2 and untreated controls identified 300 cDNA whose expression levels were significantly associated with E2 treatment (FDR < 1%) and exhibited a > 1.5-fold difference in expression level. Consolidation of redundant clones resulted in 233 unique genes, of which 129 were downregulated and 104 were upregulated following E2 treatment (Tables 2

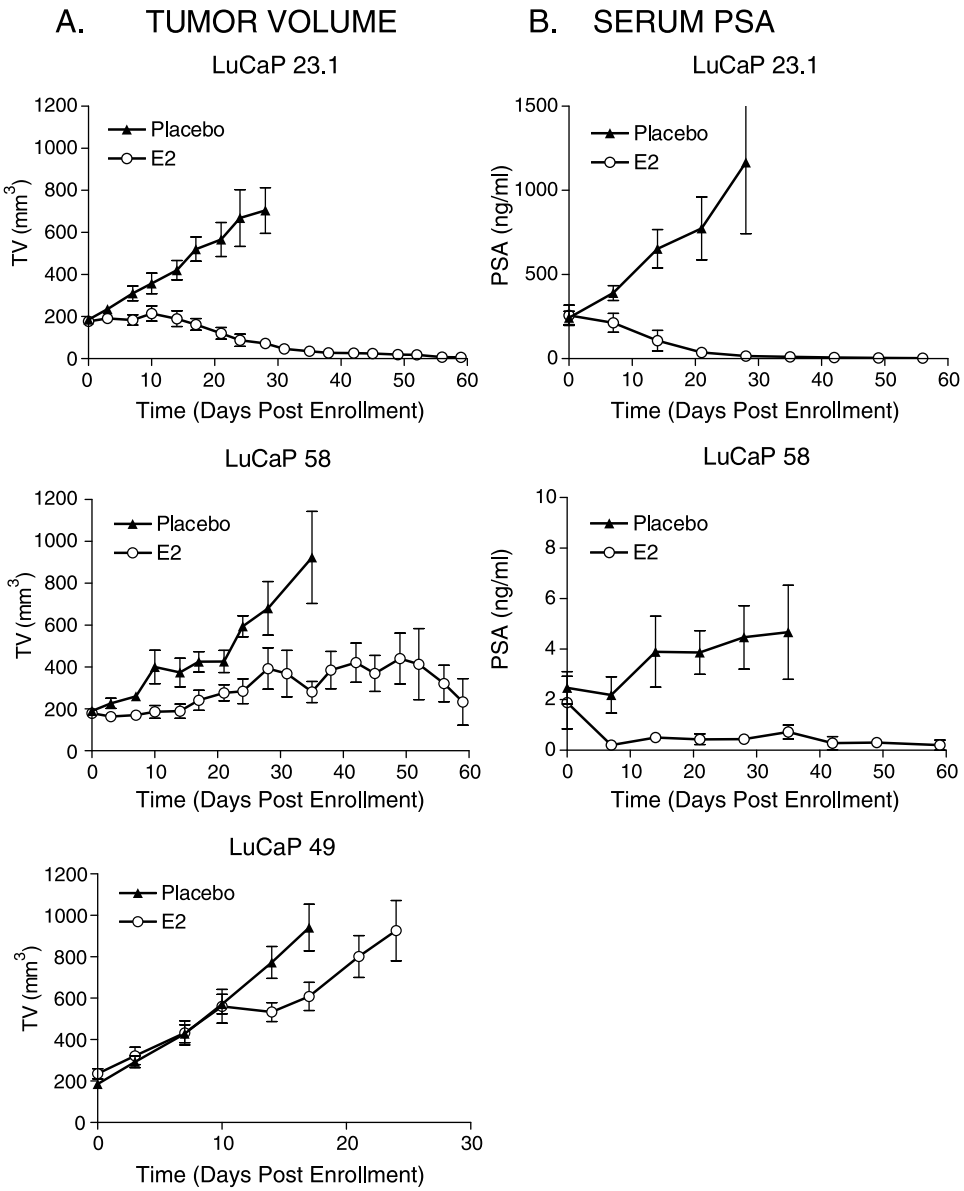

Figure 3. *Effects of E2 treatment on the growth of CaP xenografts in an androgen-free environment. LuCaP 23.1, LuCaP 49, and LuCaP 58 were implanted in castrated male mice. When tumors reached 200 to 400 mm^3, the animals were divided into two groups per xenograft: 1) placebo and 2) E2 pellet. Tumor growth and PSA were monitored as described in Materials and Methods section. Supplementation of E2 inhibited the growth of all three xenografts. (A) Tumor volume. (B) PSA serum levels.*

Table 2. Genes Upregulated in E2-Treated LuCaP 35V *versus* Untreated LuCaP 35V.

Human Genome Organization Gene	Name	GenBank	Entrez Gene	Average Fold Δ	Gene List
Metabolism					
Carbohydrate					
Lyzs	Lysozyme (*Mus musculus*)	M21050	17105	2.9	
SIAT1	Sialyltransferase 1	NM_173217	6480	2.7	
EXT1	Exostoses 1	BQ021387	2131	1.8	
Lipid/sterol					
UGT2B15	UDP glycosyltransferase 2 family, polypeptide B15	AF180322	7366	3.7	
SORL1	Sortilin-related receptor, L (DLR class) A repeats–containing	AK096577	6653	2.4	
PSAP	Prosaposin	CR617297	5660	1.9	
APOE	Apolipoprotein E	BG715607	348	1.8	
CLN2	Ceroid lipofuscinosis, neuronal 2, late infantile	AF017456	1200	1.8	
Protein					
FOLH1	Folate hydrolase (prostate-specific membrane antigen) 1	BC025672	2346	3.6	
SQSTM1	Sequestosome 1	BQ220165	8878	1.8	
DDC	Dopa decarboxylase	CA488364	1644	1.8	
MAOA	Monoamine oxidase A	NM_000240	4128	1.5	
Other					
SOD2	Superoxide dismutase 2, mitochondrial	BU527631	6648	1.9	
VKORC1	Vitamin K epoxide reductase complex, subunit 1	NM_024006	79001	1.7	
TBC1D14	TBC1 domain family, member 14	AL833868	57533	1.5	
Immune response					
CD74	CD74 antigen	CA437013	972	5.1	
HLA DRA	MHC, class II, DR α	BG757515	3122	3.4	
HLA F	MHC, class I, F	AK096962	3134	3.0	
LGALS3BP	Lectin, galactoside-binding, soluble, 3–binding protein	BQ883924	3959	2.6	
HLA DQB1	MHC, class II, DQ β_1	L34104	3119	2.5	
HLA C	MHC, class I, C	X67818	3107	2.4	
HLA B	MHC, class I, B	AK124160	3106	2.3	IFN
HLA A	MHC, class I, A	AK027084	3105	2.2	IFN
IFITM3	IFN-induced transmembrane protein 3	BQ441207	10410	2.1	
BST2	Bone marrow stromal cell antigen 2	BQ053580	684	2.0	IFN
β2M	β_2-Microglobulin	BM453762	567	1.9	AR, IFN
CD59	CD59 antigen p18–20	BM550387	966	1.8	
IFIT1	IFN-induced protein with tetratricopeptide repeats 1	BI670242	3434	1.8	IFN
IRF1	IFN-regulatory factor 1	CR594837	3659	1.8	IFN
IFI27	IFNα-inducible protein 27	BM998410	3429	1.5	IFN
Proliferation/differentiation/apoptosis					
NDRG4	NDRG family member 4	AB021172	65009	2.8	
BCCIP	BRCA2 and CDKN1A-interacting protein	BQ421346	56647	1.7	
BIRC3	Baculoviral IAP repeat–containing 3	BC037420	330	1.7	AR
TMBIM1	Transmembrane BAX inhibitor motif–containing 1	AK130380	64114	1.6	
AGR2	Anterior gradient 2 homolog	BQ685832	10551	1.6	AR
UNC13B	Unc-13 homolog B	NM_006377	10497	1.6	
TM4SF13	Transmembrane 4 superfamily member 13	AK093487	27075	1.6	
NPM1	Nucleophosmin	CN404150	4869	1.6	
NDRG1	N-myc downstream–regulated gene 1	CR600627	10397	1.5	AR
KIAA0971	KIAA0971 protein	CD671614	22868	1.5	
Signal transduction					
HSPA1A	Heat shock 70 kDa protein 1A	CR605852	3303	7.3	
IFITM1	IFN-induced transmembrane protein 1	BQ219055	8519	2.8	IFN
LY6E	Lymphocyte antigen 6 complex, locus E	U42376	4061	2.2	
STAT1	Signal transducer and activator of transcription 1, 91 kDa	BG678000	6772	1.9	IFN
ARHGAP5	Rho GTPase-activating protein 5	BG260763	394	1.8	
OGT	O-linked *N*-acetylglucosamine (GlcNAc) transferase	U77413	8473	1.7	
RALGPS1A	Ral guanine nucleotide exchange factor RalGPS1A	AB002349	9649	1.6	
FKBP4	FK506-binding protein 4, 59 kDa	CD613711	2288	1.5	
SH3KBP1	SH3 domain kinase–binding protein 1	AY423734	30011	1.5	
NUDT4	Nudix-type motif 4	NM_019094	11163	1.5	
Structure/adhesion/motility					
MYLK	Myosin, light polypeptide kinase	BC062755	4638	3.9	AR
MYH3	Myosin, heavy polypeptide 3, skeletal muscle, embryonic	CK824450	4621	1.8	
SPARC	Secreted protein, acidic, cysteine-rich (osteonectin)	AL547671	6678	1.8	
INA	Internexin neuronal intermediate filament protein, α	CR591335	9118	1.6	
CLDN4	Claudin 4	BC000671	1364	1.5	
LAMB2	Laminin, β_2	AI754927	3913	1.5	

Table 2. (*continued*)

Human Genome Organization Gene	Name	GenBank	Entrez Gene	Average Fold Δ	Gene List
Transcription regulation					
ID1	Inhibitor of DNA-binding 1, dominant-negative helix–loop–helix protein	BM973065	3397	2.7	
HIST1H2AC	Histone 1, H2ac	BC050602	8334	2.3	
PMF1	Polyamine-modulated factor 1	BC050735	11243	2.0	
NONO	Non-POU domain–containing, octamer binding	BG171743	4841	1.9	
ZNFX1	Zinc finger, NFX1 type–containing 1	AB037825	57169	1.7	
NFAT5	Nuclear factor of activated T-cells 5, tonicity-responsive	NM_006599	10725	1.7	
NOLC1	Nucleolar and coiled-body phosphoprotein 1	BE908347	9221	1.7	
TRIM22	Tripartite motif–containing 22	AW080955	10346	1.7	AR, IFN
GPBP1	GC-rich promoter–binding protein 1	AL161991	65056	1.6	
ADAR	Adenosine deaminase, RNA-specific	U18121	103	1.5	IFN
Translation–protein synthesis					
HSP90AA2	Heat shock protein 90 kDa α, class A member 2	BC001695	3324	2.1	
DNAJB1	DnaJ (Hsp40) homolog, subfamily B, member 1	BC002352	3337	1.9	
GOLPH4	Golgi phosphoprotein 4	AA447271	27333	1.8	
DNAJA1	DnaJ (Hsp40) homolog, subfamily A, member 1	BQ221194	3301	1.8	
EIF4A2	Eukaryotic translation initiation factor 4A, isoform 2	BT009860	1974	1.7	
RPL23AP7	Ribosomal protein L23a pseudogene 7	X92108	118433	1.6	
UBC	Ubiquitin C	AK129749	7316	1.5	AR
Transport					
SELENBP1	Selenium-binding protein 1	BC009084	8991	2.9	
APBA2	Amyloid β (A4) precursor protein–binding, family A, member 2	BC082986	321	2.6	
FLJ39822	Hypothetical protein FLJ39822	CA390853	151258	2.0	
SLC12A2	Solute carrier family 12, member 2	AF439152	6558	2.0	
FLJ39822	Hypothetical protein FLJ39822	AC019197	151258	1.9	
C6orf29	Chromosome 6 open reading frame 29	AY358457	80736	1.9	
ATP1B1	ATPase, Na^+/K^+ transporting, β_1 polypeptide	NM_001677	481	1.7	
ATP6V1A	ATPase, H^+ transporting, lysosomal 70 kDa, V1 subunit A	BC012169	523	1.7	
FLJ10618	Hypothetical protein FLJ10618	AL049246	55186	1.5	
NPC2	Niemann-Pick disease, type C2	CR608935	10577	1.5	
NAPA	*N*-ethylmaleimide–sensitive factor attachment protein, α	BC007432	8775	1.5	
ATP6AP2	ATPase, H^+ transporting, lysosomal accessory protein 2	BI491181	10159	1.5	
SLC25A26	Solute carrier family 25, member 26	AJ580932	115286	1.5	
Other/unknown					
MUC13	Mucin 13, epithelial transmembrane	AK000070	56667	3.9	
SAMD9L	Sterile α motif domain–containing 9–like	BC038974	219285	3.8	
	Transcribed locus	CD103928		2.8	
	Transcribed locus, strongly similar to XP_496055.1 (predicted: similar to p40)	AW452111		2.3	
C1orf43	Chromosome 1 open reading frame 43	BQ900746	25912	1.9	
C1orf80	Chromosome 1 open reading frame 80	BC015535	64853	1.8	
SERINC3	Serine incorporator 3	BI518460	10955	1.8	
FAM73A	Family with sequence similarity 73, member A	AU131144	374986	1.6	
ITM2B	Integral membrane protein 2B	CR745752	9445	1.6	

and 3). E2 treatment resulted in significant increases in the expression of several genes that are involved in immune responses (Table 2). These include major histocompatibility complex (MHC) class I/II proteins, IFN-induced transmembrane protein 1 (IFITM1), IFN-induced transmembrane protein 3 (IFITM3), IFN-induced protein with tetratricopeptide repeats 1 (IFIT1), IFNα-inducible protein 27 (IFI27), and IFN-regulatory factor 1 (IRF1).

We have used GSEA to evaluate whether phenotypic changes caused by E2 treatment in LuCaP 35V were associated with enrichment for IFN-regulated, androgen-regulated, and estrogen-regulated genes. Our analysis showed a significant enrichment of IFN-regulated genes in E2-treated LuCaP 35V tumors (NOM $P < .001$), which remained significant when adjusted for gene set size and multiple hypothesis testing (FDR = 11.0%) (Figure 4*A*). Significant enrichment was also detected when the androgen deprivation–downregulated gene set was compared to our results (NOM $P < .001$); this enrichment also remained significant when adjusted for gene set size and multiple hypothesis testing (FDR = 21.3%) (Figure 4*B*). Estrogen-regulated genes were also enriched in phenotypic alterations after E2 treatment (NOM $P < .001$); however, these changes were not significant when adjusted for gene set size and multiple hypothesis testing (FDR = 54.5%). We hypothesize that this is due to the fact that changes in the expression of these genes occur in both up and down directions, and also due to inclusion in the list of genes that are altered in breast cancer, which may not be relevant to this study (Figure 4*C*).

Table 3. Genes Downregulated in E2-Treated LuCaP 35V *Versus* Untreated LuCaP 35V.

Human Genome Organization Gene	Name	GenBank	Entrez Gene	Average Fold Δ	Gene List
Metabolism					
Carbohydrate					
UGDH	UDP glucose dehydrogenase	BC022781	7358	−2.0	
GALNT7	UDP *N*-acetyl-α-D-galactosamine	BM976847	51809	−1.8	
GPI	Glucose phosphate isomerase	AI124792	2821	−1.8	
RPN1	Ribophorin I	CD644128	6184	−1.8	AR
SORD	Sorbitol dehydrogenase	BC025295	6652	−1.6	AR
GRHPR	Glyoxylate reductase/hydroxypyruvate reductase	BE728720	9380	−1.5	
ACLY	ATP citrate lyase	BI869432	47	−1.5	
Lipid/sterol					
RODH	3-Hydroxysteroid epimerase	AF223225	8630	−9.5	
FACL3	Fatty acid–coenzyme A ligase, long-chain 3	AK023191	2181	−3.0	
TMEPAI	Transmembrane, prostate androgen–induced RNA	NM_199170	56937	−2.6	AR
PPAP2A	Phosphatidic acid phosphatase type 2A	CR617429	8611	−2.5	
EBP	Emopamil-binding protein (sterol isomerase)	CN395741	10682	−2.2	AR
DHCR24	24-Dehydrocholesterol reductase	BC011669	1718	−2.1	AR
PIGF	Phosphatidylinositol glycan, class F	BQ006858	5281	−2.1	
CERK	Ceramide kinase	NM_182661	64781	−1.5	
Protein					
HMGCS2	3-Hydroxy-3-methylglutaryl–coenzyme A synthase 2	NM_005518	3158	−2.9	AR
MME	Membrane metalloendopeptidase	AL833459	4311	−2.3	
KLK3	Kallikrein 3, (PSA)	CF140712	354	−2.3	AR, IFN
ODC1	Ornithine decarboxylase 1	BU153337	4953	−1.9	AR
GOT2	Glutamic–oxaloacetic transaminase 2, mitochondrial	AK098313	2806	−1.7	
ACY1L2	Aminoacylase 1–like 2	AK094996	135293	−1.7	
GBDR1	Putative glioblastoma cell differentiation-related	BC004967	10422	−1.7	
ADAM23	A disintegrin and metalloproteinase domain 23	AF052115	8745	−1.7	
ALDH1A3	Aldehyde dehydrogenase 1 family, member A3	BX538027	220	−1.6	AR
KLK2	Kallikrein 2, prostatic	NM_005551	3817	−1.6	AR
GOT1	Glutamic–oxaloacetic transaminase 1, soluble	CR616132	2805	−1.5	AR
Other					
NDUFS3	NADH dehydrogenase (ubiquinone) Fe–S protein 3, 30 kDa	AF100743	4722	−2.1	
ACPP	Acid phosphatase, prostate	AI547266	55	−2.1	AR
DTYMK	Deoxythymidylate kinase	AA427388	1841	−2.1	
DCXR	Dicarbonyl/L-xylulose reductase	BM795570	51181	−1.6	
RRM1	Ribonucleotide reductase M1 polypeptide	AK122695	6240	−1.6	
AK3	Adenylate kinase 3	AW014145	205	−1.6	
NME1	Nonmetastatic cells 1, protein (NM23A)	NM_000269	4830	−1.6	E2
Proliferation/differentiation/apoptosis					
CCDC5	Coiled coil domain–containing 5	AI142429	115106	−2.0	
TPT1	Tumor protein, translationally controlled 1	AU119000	7178	−1.7	
MAD2L1	MAD2 mitotic arrest deficient–like 1	BC005945	4085	−1.6	
PCNA	Proliferating cell nuclear antigen	AA953221	5111	−1.6	
CCNG2	Cyclin G2	CR598707	901	−1.6	
MCM3	MCM3 minichromosome maintenance-deficient 3	BQ213935	4172	−1.5	
Signal transduction					
FKBP5	FK506-binding protein 5	BU618502	2289	−2.7	AR
RACGAP1	Rac GTPase–activating protein 1	AB040911	29127	−2.2	
STMN1	Stathmin 1/oncoprotein 18	BM543057	3925	−2.0	
CAMKK2	Calcium/calmodulin–dependent protein kinase kinase 2, β	NM_006549	10645	−2.0	AR
MAP2K1	Mitogen-activated protein kinase kinase 1	L05624	5604	−1.9	IFN
RAB27A	RAB27A, member *RAS* oncogene family	U38654	5873	−1.9	
GNB2L1	Guanine nucleotide–binding protein (G protein), β polypeptide 2–like 1	BE300778	10399	−1.8	
MAP2K4	Mitogen-activated protein kinase kinase 4	NM_003010	6416	−1.7	
SLC9A3R2	Solute carrier family 9, isoform 3 regulatory factor 2	BU540416	9351	−1.7	
TM4SF3	Transmembrane 4 superfamily member 3	NM_004616	7103	−1.6	
APPBP1	Amyloid β precursor protein–binding protein 1, 59 kDa	BC041323	8883	−1.6	
CCL2	Chemokine (C–C motif) ligand 2	BU532858	6347	−1.6	
RAN	RAN, member *RAS* oncogene family	BG775164	5901	−1.5	
Structure/adhesion/motility					
DKFZP761D0211	Hypothetical protein DKFZp761D0211	CR619764	83986	−2.1	
COL1A1	Collagen, type I, α_1	CV799740	1277	−2.1	
HMMR	Hyaluronan-mediated motility receptor	CR601287	3161	−2.0	
COL2A1	Collagen, type II, α_1	CX119275	1280	−1.8	
TSPAN-1	Tetraspan 1	CA454232	10103	−1.7	
Postn	periostin, osteoblast-specific factor (*M. musculus*)	BC031449	50706	−1.7	
LCP1	Lymphocyte cytosolic protein 1	BC015001	3936	−1.7	
MYBPC1	Myosin-binding protein C, slow type	BF516586	4604	−1.6	

Table 3. (*continued*)

Human Genome Organization Gene	Name	GenBank	Entrez Gene	Average Fold Δ	Gene List
Structure/adhesion/motility					
SMOC1	SPARC-related modular calcium-binding 1	CD049369	64093	−1.6	
NUP93	Nucleoporin 93 kDa	CR612078	9688	−1.6	
SYNPO2	Synaptopodin 2	AL833547	171024	−1.5	
CKAP5	Cytoskeleton-associated protein 5	CR623748	9793	−1.5	
CXCR4	Chemokine (C−X−C motif) receptor 4	BF591711	7852	−1.5	
Transcription regulation					
NKX3-1	NK3 transcription factor−related, locus 1	BX102941	4824	−3.3	
SPDEF	SAM-pointed domain−containing ets transcription factor	BG328411	25803	−2.5	
TOP2A	Topoisomerase (DNA) II α 170 kDa	AW172827	7153	−2.3	E2
CREB3L4	cAMP-responsive element−binding protein 3−like 4	AF394167	148327	−2.3	
H2AFZ	H2A histone family, member Z	BU178992	3015	−1.9	
RFC3	Replication factor C3, 38 kDa	BC000149	5983	−1.9	
CDK2AP1	CDK2-associated protein 1	BU608264	8099	−1.8	
SMARCA2	SWI/SNF-related, matrix-associated, actin-dependent regulator of chromatin, subfamily a, member 2	BM671383	6595	−1.6	
SMC2L1	SMC2 structural maintenance of chromosomes 2−like 1	BC032705	10592	−1.5	
SNRPB	Small nuclear ribonucleoprotein polypeptides B and B1	BX363533	6628	−1.5	
RAD51C	RAD51 homolog C	AW270829	5889	−1.5	
HIRIP3	HIRA-interacting protein 3	NM_003609	8479	−1.5	
Translation−protein synthesis					
GOLPH2	Golgi phosphoprotein 2	AW591201	51280	−2.6	
RPS2	Ribosomal protein S2	CR610190	6187	−2.3	
RPL4	Ribosomal protein L4	BM451248	6124	−2.2	
NAG	Neuroblastoma-amplified protein	NM_015909	51594	−2.1	
LOC388817	Peptidylprolyl isomerase A−like	BM972350	388817	−2.1	
LRIG1	Leucine-rich repeats and immunoglobulin-like domains 1	BC014276	26018	−2.0	
EEF1A1	Eukaryotic translation elongation factor 1 α_1	BC020477	1915	−1.9	
RPS8	Ribosomal protein S8	BQ218087	6202	−1.9	
RAI14	Retinoic acid−induced 14	AY317139	26064	−1.8	
RPL6	Ribosomal protein L6	BC071912	6128	−1.8	
RPL9	Ribosomal protein L9	BQ961538	6133	−1.8	
RPL10A	Ribosomal protein L10a	BQ941098	4736	−1.7	
EEF1B2	Eukaryotic translation elongation factor 1 β_2	BX353697	1933	−1.7	
RPS6	Ribosomal protein S6	BG029552	6194	−1.6	
RPL26	Ribosomal protein L26	BG925676	6154	−1.6	
RPL31	Ribosomal protein L31	CN269893	6160	−1.6	
RPL5	Ribosomal protein L5	BM721056	6125	−1.6	
NACA	Nascent polypeptide−associated complex α polypeptide	BU164695	4666	−1.6	
RPL13A	Ribosomal protein L13a	BQ229130	23521	−1.6	
EIF3S6IP	Eukaryotic translation initiation factor 3, subunit 6−interacting protein	BX424780	51386	−1.6	
RPL11	Ribosomal protein L11	BU902342	6135	−1.6	
RPS3A	Ribosomal protein S3A	BM463771	6189	−1.5	
RPS15A	Ribosomal protein S15a	CN351294	6210	−1.5	
RPLP0	Ribosomal protein, large, P0	BG575128	6175	−1.5	
RPS13	Ribosomal protein S13	CA843734	6207	−1.5	
RPL10	Ribosomal protein L10	BM423499	6134	−1.5	
RPS4X	Ribosomal protein S4, X-linked	BQ959684	6191	−1.5	
Transport					
DBI	Diazepam-binding inhibitor	BQ940531	1622	−2.5	
VPS45A	Vacuolar protein sorting 45A	AK023170	11311	−2.2	
HBE1	Hemoglobin, epsilon 1	AA115963	3046	−2.0	
SLC39A6	Solute carrier family 39, member 6	BC008317	25800	−1.7	
RAB3B	RAB3B, member *RAS* oncogene family	BF792558	5865	−1.7	
KPNA2	Karyopherin α_2	U09559	3838	−1.6	
TOMM40	Translocase of outer mitochondrial membrane 40 homolog	BQ883428	10452	−1.6	
SLC16A1	Solute carrier family 16, member 1	AK000641	6566	−1.6	AR
SLC25A3	Solute carrier family 25, member 3	BC068067	5250	−1.5	
ATP5B	ATP synthase, H^+-transporting, mitochondrial F1 complex, β polypeptide	CR591449	506	−1.5	
Other/unknown					
KIAA0114	KIAA0114 gene product	BI850303	57291	−2.3	
BRP44	Brain protein 44	BQ287816	25874	−2.2	
THAP5	THAP domain−containing 5	NM_182529	168451	−2.0	
HN1	Hematological and neurological expressed 1	CN363269	51155	−2.0	
KIAA0460	KIAA0460 protein	AB007929	23248	−2.0	
PRAC	Small nuclear protein PRAC	BU942850	84366	−1.8	
SURF4	Surfeit 4	CR602588	6836	−1.7	

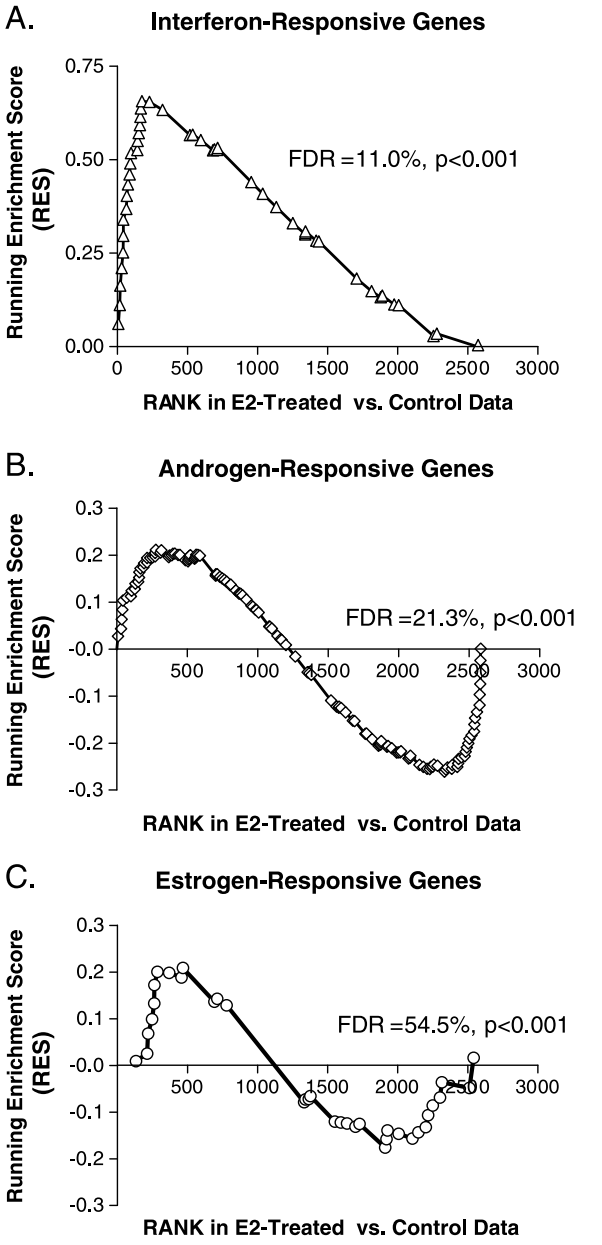

Figure 4. *Enrichment plot of gene signatures in the E2-treated LuCaP 35V data set. The plots show the locations of the IFN (A), androgen (B), and estrogen (C) signature genes in the gene set ranked by the E2 phenotype. The running enrichment score (RES), as a function of position in the gene list, is shown. The signal-to-noise ranks of all 2584 genes in the gene set are shown, with low ranks indicating genes upregulated by E2 treatment and with high ranks indicating genes downregulated by E2 treatment. IFN signature genes are clearly overrepresented on the left side of the gene list, representing their enrichment in the genes significantly upregulated by E2 treatment (FDR = 11.0%). Androgen signature genes are present on both sides of the gene list, representing their enrichment in the genes significantly downregulated and upregulated by E2 treatment (FDR = 21.3%). Estrogen signature genes are also clustered on both ends of the ranked list, representing upregulation and downregulation by E2 treatment (FDR = 54.5%).*

ERβ Localization and DNA Binding

ERβ (55 kDa) was detected by Western blot analysis in nuclear extracts from—but not in the cytoplasm of—LuCaP 35V and E2-treated LuCaP 35V (Figure 5*A*). E2 treatment increased levels of ERβ in the nucleus by approximately 30%. Using EMSA, we showed that ERβ in the nucleus is able to bind to DNA. E2 treatment slightly increased levels of ERβ/DNA complexes (Figure 5*B*). The specificity of the interaction was demonstrated by the disappearance of the specific band in control reactions with a mutated ERE (xERE).

Determination of E2-Mediated Alterations in Tumor Gene Expression by qRT-PCR

We performed qRT-PCR analysis to confirm the cDNA microarray results for selected genes of potential biologic importance. All messages whose expression was determined to be upregulated by cDNA array analysis were also increased by qRT-PCR in E2-treated LuCaP 35V (Figure 6). We next examined whether immune response–related genes found to be upregulated by E2 treatment of LuCaP 35V xenografts were also altered by E2 treatment in other CaP xenografts. In LuCaP 58, the patterns of E2 alteration in the expression of these genes were similar to those in LuCaP 35V. In contrast, in LuCaP 49 (a neuroendocrine CaP xenograft whose growth suppression was less pronounced), the expression of evaluated genes was minimally altered (Figure 6). LuCaP 23.1 regressed almost completely after E2 treatment, and, unfortunately, there was insufficient tissue remaining for analysis. Gene expression changes in LuCaP 35 tumors treated with E2 or DES after castration were also evaluated. We found that the expression of genes related to immune regulation was altered by E2 and DES treatment, as in LuCaP 35V tumors. We continued to examine tumor gene expression levels after expiration of the E2 pellets and found that levels of E2-induced messages decreased, indicating dependence on the presence of E2 (Figure 7).

Discussion

Several studies dating back to the 1980s have suggested that mechanisms other than androgen suppression may be involved in the estrogen-mediated inhibition of CaP growth. Estrogens appear to be slightly more effective in treating CaP than other means of androgen suppression [4]. Compounds with estrogenic activity are capable of exerting direct cytotoxic effects on androgen-independent CaP cells *in vitro* [19–23]. Our data, obtained from the androgen-deficient environment of female mice [24] and from the present work, show that estrogens have powerful growth-inhibitory effects on CaP *in vivo*.

In the present study, we have shown that E2 and DES both inhibit the growth of androgen-independent CaP tumors in the androgen-depleted environment of castrated male mice. These data clearly demonstrate that E2 exhibits effects on CaP cells that are unrelated to the suppression of the hypothalamic–hypophyseal axis and the subsequent decrease in testosterone. This novel observation prompted us to characterize the effects of E2 on androgen-independent CaP at the molecular level by profiling transcript alterations. Although many of the genes differentially regulated by estrogen in this system are of unclear significance, others have quite plausible roles in the observed growth inhibition on the basis of their established functions. Among these are genes

involved in signal transduction, cellular metabolism, and the control of transcription and translation. We also observed substantial changes in genes that function to regulate immune responses—a mechanism that may contribute to tumor growth–inhibitory effects resulting from estrogen treatment.

Among immune response–related genes altered by E2 treatment in CaP are those modulating cellular responses to IFNs. This group was found to be significantly enriched in the set of genes upregulated by E2 when tested by GSEA using an independently generated list of IFN-regulated genes. The increased expression of IFN-regulated genes is of particular interest due to the direct antitumor activities reported for these cytokines [43–50]. Our results are in keeping with the results on the upregulation of IFN-regulated genes in LNCaP CaP cells following exposure to the estrogenic herbal preparation PC-SPES [51] and the induction of IFNγ-regulated genes after E2 treatment in other tissues [52]. In addition, tamoxifen has been shown to enhance IFN-regulated gene expression in breast cancer cells [53]. Specifically, IRF1, whose expression was increased three-fold by E2 (qRT-PCR data), has been described as a negative regulator of proliferation [54] and has exhibited tumor-suppressor activities in breast cancer cells [55]. These published observations and our results are consistent with a model in which IFN and genes regulated by IFN modulate a component of the growth-inhibitory activity of E2 toward androgen-independent CaP cells.

E2 treatment significantly increased the expression of several MHC class I/II transcripts in the androgen-independent LuCaP 35V xenograft. Similarly, the upregulation of MHC class I transcripts has been observed in LNCaP cells on PC-SPES exposure [51]. MHC class I molecules are expressed in most human cells and play a pivotal role in the immune response to viruses and tumor cells. Tumor cells often evolve mechanisms to modulate or escape immune surveillance through the downregulation of MHC class I molecules [56–60]. IFNγ treatment, like E2 treatment in our studies, has been reported to upregulate the expression of MHC class I/II molecules in CaP cell lines [44,58,59]. According to this evidence, the treatment of advanced CaP patients with E2 might result not only in direct inhibitory effects but also in the stimulation of T-cell attack on tumors by the upregulation of MHC proteins. Such a mechanism could not be directly tested in our study, which employed immune-compromised SCID mice, but it represents an independent potential benefit of E2 treatment that could be exploited in the context of clinical therapies employing vaccine or other immunomodulatory treatment strategies.

DES has been reported to be ineffective in inhibiting LuCaP 35 growth in intact male mice [61]. We also observed that E2 did not inhibit LuCaP 35 growth in intact male mice (data not shown). These results suggest that phenotypic changes caused by E2 treatment are specific to an androgen-depleted environment. In contrast to our E2 data, raloxifene, an estrogen receptor antagonist, has been reported to inhibit the growth of both androgen-sensitive and androgen-independent CaP *in vitro* [20,21]. Raloxifene has also been reported to delay CaP development in probasin/SV40 T antigen transgenic rats [62] and to inhibit the growth of both androgen-sensitive and androgen-independent variants of the CWR22 CaP xenograft [63]. Thus, the emerging picture of estrogenic effects on androgen-independent CaP is complex, possibly involving multiple mechanisms, some of which may involve signal transduction by estrogen receptors. Additional preclinical studies are clearly warranted to deconvolute these effects.

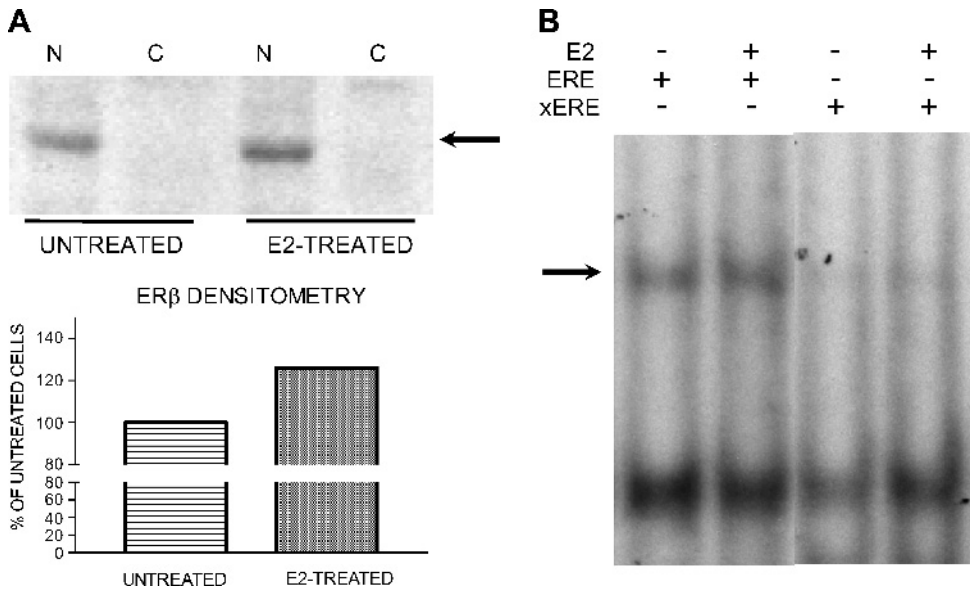

Figure 5. *Measurements of ERβ expression in LuCaP 35V xenografts. LuCaP 35 cells were isolated from tumor bits and treated in vitro with E2 for 4 hours. (A) ERβ was detected in nuclear extracts, whereas cytoplasmic protein extracts were negative for ERβ. E2 increased the amount of ERβ in the nucleus by ~ 1.5-fold. (B) Nuclear extracts of LuCaP 35V and LuCaP 35V that were treated with E2 in vitro for 4 hours were used for EMSA. ERβ/DNA complexes were detected in both samples, with increased amounts in E2-treated LuCaP 35V. The specificity of binding was demonstrated by competition with an xERE sequence.*

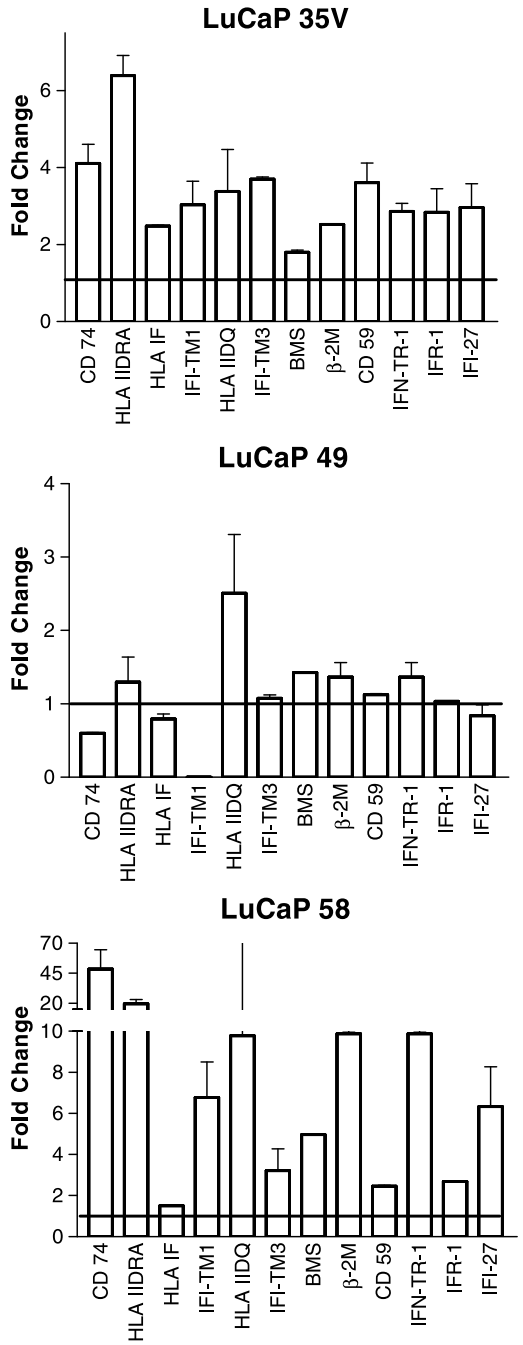

Figure 6. *qRT-PCR analysis of the expression of immune-related genes. Sets of pooled samples (n = 5) from control and E2-treated tumors were used for real-time PCR analyses. Data are presented as relative expression normalized to housekeeping genes, as described in Materials and Methods section. Real-time analysis confirmed the results of the cDNA array analysis of LuCaP 35V. Moreover, immune-related genes exhibited similar alterations in LuCaP 58 on E2 treatment. Alterations in these messages in LuCaP 49 were very small or undetectable, suggesting that other mechanisms are also involved in the E2 inhibition observed and that the expression of ARs may play a role in the altered expression of these messages. Results are presented as mean ± SEM of the change factor over untreated tumors.*

A potential mechanism whereby E2 may cause alterations of the gene expression profile we have observed in CaP cells is signal transduction through ERβ expressed by CaP cells. It has been reported that ERβ expression declines as CaP develops in the prostate gland, but we and others have shown that it reappears in lymph node and bone metastases [27]. This apparent discrepancy is probably explained by the recent findings of the reversible epigenetic regulation of ERβ in CaP metastases [64]. We have shown previously that the xenografts used in this study express ERβ [24]. In the present study, we have shown that the androgen-independent LuCaP 35V xenograft expresses ERβ protein in a form that is capable of DNA binding, and that ERβ levels in nuclei and DNA-binding activities are increased on E2 treatment. Together, these results suggest the possibility that E2-mediated inhibition is, at least in part, transduced by ERβ signaling, but further studies are required to demonstrate direct involvement of ERβ with these phenomena. One important aspect of preclinical testing involves the use of models that mimic the disease in patients. If it is eventually found that E2 is beneficial in advanced CaP and that the effects are mediated by ERβ, then evaluation of the expression of ERβ in patient tumors could prove to be valuable in treatment decisions, as is the case with HER2/Neu and herceptin treatment today.

The E2-inhibitory effects observed cannot be caused by suppression of the hypothalamic–hypophyseal axis reduction in testosterone levels because the tumors were grown in castrated male mice. However, our data do suggest that AR signaling may be at least partially involved in the inhibitory effects observed. All of the xenografts, except LuCaP 49, express AR (data not shown), and the inhibition of LuCaP 49 by E2 was less pronounced than in other xenografts. Moreover, GSEA showed that genes in an independently generated list of genes downregulated by androgen deprivation were significantly enriched in the phenotype of E2-treated LuCaP 35V, with about half of the genes downregulated by E2 and half upregulated by E2. For example, the expression of heat shock protein 70, which is downregulated after castration [65], was upregulated by E2 treatment (Table 2). These results illustrate the complexity of these signaling networks. Further studies are needed to delineate the action of E2 on AR signaling in CaP cells.

The results reported here support the multifaceted roles of estrogen in the inhibition of androgen-independent CaP growth. These observations extend the traditional view of estrogen activity beyond the suppression of circulating concentrations of androgens. Direct cellular effects and the modulation of immune responses represent additional potential mechanisms that could be further exploited through combination therapies. Given that estrogens also decrease bone lysis caused by androgen suppression [66] and may ameliorate cognitive side effects associated with low testosterone [67], the use of estrogens should be considered as a viable first-line treatment strategy for androgen-independent CaP.

Acknowledgements

PSA reagents were kindly provided by Abbott Laboratories. The authors would like to thank Janna Quinn and Austin Odman for excellent technical assistance, Stacy Moore for

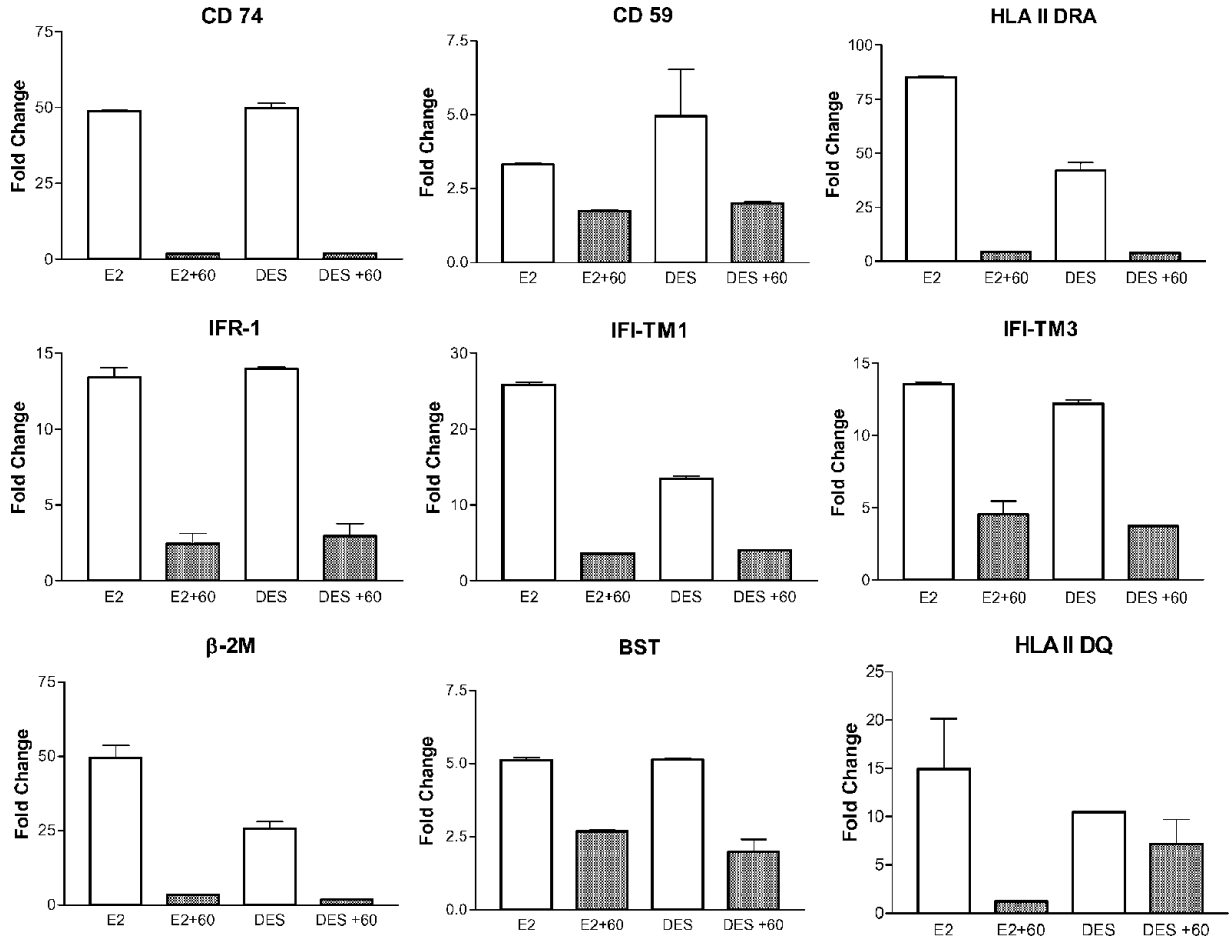

Figure 7. *Expression changes in immune-related genes following E2 or DES treatment of androgen-independent CaP xenografts. LuCaP 35 tumor bits were implanted in intact animals, and animals were castrated when tumors reached ~ 200 to 400 mm^3. At the time of the development of recurrent CaP, animals were randomized into three groups. E2 and DES pellets were implanted in treatment animals; control animals received placebo pellets. Animals were sacrificed after tumors had reached 1000 mg, 90 days after pellet implantation (E2, DES) or 60 days after pellet expiration (E2 + 60, DES + 60). RNA was extracted and qRT-PCR was performed as described in Materials and Methods section. The results show that E2 and DES treatment increased the expression of immune-related messages in a similar manner. Gene expression changes were dependent on the presence of estrogenic compounds because, after pellet expiration, the levels of these messages had decreased, in some cases nearly to levels observed in untreated animals. Data (mean ± SEM) are presented as relative expression normalized to housekeeping genes, as described in Materials and Methods section.*

help with cDNA arrays, Michael Corey for editorial assistance, and Bruce Montgomery, Bernd Stein, and Shuk-Mei Ho for helpful discussions.

References

[1] Huggins C and Hodges CV (2002). Studies on prostatic cancer: I. The effect of castration, of estrogen and of androgen injection on serum phosphatases in metastatic carcinoma of the prostate. *J Urol* **167,** 948–951.

[2] Cox RL and Crawford ED (1995). Estrogens in the treatment of prostate cancer. *J Urol* **154,** 1991–1998.

[3] de la Monte SM, Moore GW, and Hutchins GM (1986). Metastatic behavior of prostate cancer. Cluster analysis of patterns with respect to estrogen treatment. *Cancer* **58,** 985–993.

[4] Byar DP and Corle DK (1988). Hormone therapy for prostate cancer: results of the Veterans Administration Cooperative Urological Research Group studies. *Natl Cancer Inst Monogr* **7,** 165–170.

[5] Brendler H (1969). Therapy with orchiectomy or estrogens or both. *JAMA* **210,** 1074–1076.

[6] Presti JC Jr (1996). Estrogen therapy for prostate carcinoma. *JAMA* **275,** 1153.

[7] Usui T, Sagami K, Kitano T, Nihira H, and Miyachi Y (1982). The changes in the binding capacity of testosterone–oestradiol binding globulin (TeBG) following castration and DES-D administration in patients with prostatic carcinoma. *Urol Res* **10,** 119–122.

[8] Alder A, Burger H, Davis J, Dulmanis A, Hudson A, Sarfaty G, and Straffon W (1968). Carcinoma of prostate: response of plasma luteinizing hormone and testosterone to oestrogen therapy. *Br Med J* **1,** 28–30.

[9] Srinivasan G, Campbell E, and Bashirelahi N (1995). Androgen, estrogen, and progesterone receptors in normal and aging prostates. *Microsc Res Tech* **30,** 293–304.

[10] Turkes AO, Peeling WB, Wilson DW, and Griffiths K (1988). Evaluation of different endocrine approaches in the treatment of prostatic carcinoma. In H Klosterhalfen (Ed.), New Developments in Biosciences, Walter de Gruyter and Co., Berlin, pp. 75–86.

[11] The Veterans Administration Cooperative Urological Research Group (1967). Carcinoma of the prostate: treatment comparisons. *J Urol* **98,** 516–522.

[12] The Veterans Administration Cooperative Urological Research Group (1967). Treatment and survival of patients with cancer of the prostate. *Surg Gynecol Obstet* **124,** 1011–1017.

[13] Bailar JDI and Byar DP (1970). Estrogen treatment for cancer of the prostate. Early results with 3 doses of diethylstilbestrol and placebo. *Cancer* **26,** 257.

[14] Cox RL and Crawford ED (1995). Estrogens in the treatment of prostate cancer. *J Urol* **154,** 1991–1998.

[15] Burns-Cox N, Basketter V, Higgins B, and Holmes S (2002). Prospective randomised trial comparing diethylstilbestrol and flutamide in the treatment of hormone relapsed prostate cancer. *Int J Urol* **9,** 431–434.

[16] Leav I, Lau KM, Adams JY, McNeal JE, Taplin ME, Wang J, Singh H, and Ho SM (2001). Comparative studies of the estrogen receptors beta and alpha and the androgen receptor in normal human prostate glands, dysplasia, and in primary and metastatic carcinoma. *Am J Pathol* **159,** 79–92.

[17] Pasquali D, Staibano S, Prezioso D, Franco R, Esposito D, Notaro A, De Rosa G, Bellastella A, and Sinisi AA (2001). Estrogen receptor beta expression in human prostate tissue. *Mol Cell Endocrinol* **178,** 47–50.

[18] Lau KM, LaSpina M, Long J, and Ho SM (2000). Expression of estrogen receptor (ER)-alpha and ER-beta in normal and malignant prostatic epithelial cells: regulation by methylation and involvement in growth regulation. *Cancer Res* **60,** 3175–3182.

[19] Carruba G, Pfeffer U, Fecarotta E, Coviello DA, D'Amato E, Lo Castro M, Vidali G, and Castagnetta L (1994). Estradiol inhibits growth of hormone-nonresponsive PC3 human prostate cancer cells. *Cancer Res* **54,** 1190–1193.

[20] Kim IY, Kim BC, Seong DH, Lee DK, Seo JM, Hong YJ, Kim HT, Morton RA, and Kim SJ (2002). Raloxifene, a mixed estrogen agonist/antagonist, induces apoptosis in androgen-independent human prostate cancer cell lines. *Cancer Res* **62,** 5365–5369.

[21] Kim IY, Seong DH, Kim BC, Lee DK, Remaley AT, Leach F, Morton RA, and Kim SJ (2002). Raloxifene, a selective estrogen receptor modulator, induces apoptosis in androgen-responsive human prostate cancer cell line LNCaP through an androgen-independent pathway. *Cancer Res* **62,** 3649–3653.

[22] L'Esperance JO and Mobley J (2002). A novel estrogenic compound induces apoptosis–necrosis through an estrogen-receptor-β pathway, in the DU145 prostate cancer cell line. *J Urol* **167,** 49.

[23] Mobley JA, L'Esperance JO, Wu M, Friel CJ, Hanson RH, and Ho SM (2004). The novel estrogen 17alpha-20*Z*-21-[(4-amino)phenyl]-19-norpregna-1,3,5(10),20-tetraene-3,17beta-estradiol induces apoptosis in prostate cancer cell lines at nanomolar concentrations *in vitro*. *Mol Cancer Ther* **3,** 587–595.

[24] Corey E, Quinn JE, Emond MJ, Buhler KR, Brown LG, and Vessella RL (2002). Inhibition of androgen-independent growth of prostate cancer xenografts by 17 beta-estradiol. *Clin Cancer Res* **8,** 1003–1007.

[25] Horvath LG, Henshall SM, Lee CS, Head DR, Quinn DI, Makela S, Delprado W, Golovsky D, Brenner PC, O'Neill G, et al. (2001). Frequent loss of estrogen receptor-beta expression in prostate cancer. *Cancer Res* **61,** 5331–5335.

[26] Fujimura T, Takahashi S, Urano T, Ogawa S, Ouchi Y, Kitamura T, Muramatsu M, and Inoue S (2001). Differential expression of estrogen receptor beta (ERbeta) and its C-terminal truncated splice variant ERbetacx as prognostic predictors in human prostatic cancer. *Biochem Biophys Res Commun* **289,** 692–699.

[27] Lai JS, Brown LG, True LD, Hawley SH, Etzioni R, Higano CS, Ho SM, Vessella RL, and Corey E (2004). Metastases of prostate cancer express estrogen receptor beta. *Urology* **64,** 814–820.

[28] Corey E, Quinn JE, Buhler KR, Nelson PS, Macoska JA, True LD, and Vessella RL (2003). LuCaP 35: a new model of prostate cancer progression to androgen independence. *Prostate* **55,** 239–246.

[29] Ellis WJ, Vessella RL, Buhler KR, Bladou F, True LD, Bigler SA, Curtis D, and Lange PH (1996). Characterization of a novel androgen-sensitive, prostate-specific antigen–producing prostatic carcinoma xenograft: LuCaP 23. *Clin Cancer Res* **2,** 1039–1048.

[30] Bladou F, Vessella RL, Buhler KR, Ellis WJ, True LD, and Lange PH (1996). Cell proliferation and apoptosis during prostatic tumor xenograft involution and regrowth after castration. *Int J Cancer* **67,** 785–790.

[31] Corey E and Vessella RL (2006). Xenograft models of human prostate cancer, in: Prostate Cancer: novel biology, genetics and therapy, 2nd edition, LWK Chung and ET Keller (Eds.), Human Press, Totowa, NJ, 2006.

[32] True LD, Buhler KR, Quinn J, Williams E, Nelson P, Clegg N, Macoska JA, Norwood T, Liu A, Ellis W, et al. (2002). A neuroendocrine/small cell prostate carcinoma xenograft: LuCaP 49. *Am J Pathol* **161,** 705–715.

[33] Brubaker KD, Vessella RL, Brown LG, and Corey E (2003). Prostate cancer expression of runt-domain transcription factor Runx2, a key regulator of osteoblast differentiation and function. *Prostate* **56,** 13–22.

[34] Hawkins V, Doll D, Bumgarner R, Smith T, Abajian C, Hood L, and Nelson PS (1999). PEDB: the prostate expression database. *Nucleic Acids Res* **27,** 204–208.

[35] Nelson PS, Clegg N, Eroglu B, Hawkins V, Bumgarner R, Smith T, and Hood L (2000). The prostate expression database (PEDB): status and enhancements in 2000. *Nucleic Acids Res* **28,** 212–213.

[36] Nelson PS, Pritchard C, Abbott D, and Clegg N (2002). The human (PEDB) and mouse (mPEDB) prostate expression databases. *Nucleic Acids Res* **30,** 218–220.

[37] Nelson PS, Clegg N, Arnold H, Ferguson C, Bonham M, White J, Hood L, and Lin B (2002). The program of androgen-responsive genes in neoplastic prostate epithelium. *Proc Natl Acad Sci USA* **99,** 11890–11895.

[38] Tusher VG, Tibshirani R, and Chu G (2001). Significance analysis of microarrays applied to the ionizing radiation response. *Proc Natl Acad Sci USA* **98,** 5116–5121.

[39] Ashburner M, Ball CA, Blake JA, Botstein D, Butler H, Cherry JM, Davis AP, Dolinski K, Dwight SS, Eppig JT, et al. (2000). Gene ontology: tool for the unification of biology. The Gene Ontology Consortium. *Nat Genet* **25,** 25–29.

[40] Subramanian A, Tamayo P, Mootha VK, Mukherjee S, Ebert BL, Gillette MA, Paulovich A, Pomeroy SL, Golub TR, Lander ES, et al. (2005). Gene Set Enrichment Analysis: a knowledge-based approach for interpreting genome-wide expression profiles. *Proc Natl Acad Sci USA* **102,** 15545–15550.

[41] DePrimo SE, Diehn M, Nelson JB, Reiter RE, Matese J, Fero M, Tibshirani R, Brown PO, and Brooks JD (2002). Transcriptional programs activated by exposure of human prostate cancer cells to androgen. *Genome Biol* **3,** RESEARCH0032.

[42] Vandesompele J, De Preter K, Pattyn F, Poppe B, Van Roy N, De Paepe A, and Speleman F (2002). Accurate normalization of real-time quantitative RT-PCR data by geometric averaging of multiple internal control genes. *Genome Biol* **3,** RESEARCH0034.

[43] Kominsky SL, Hobeika AC, Lake FA, Torres BA, and Johnson HM (2000). Down-regulation of neu/HER-2 by interferon-gamma in prostate cancer cells. *Cancer Res* **60,** 3904–3908.

[44] Sokoloff MH, Tso C-L, Kaboo R, Taneja S, Pang S, DeKernion JB, and Belldegrun AS (1996). *In vitro* modulation of tumor progression-associated properties of hormone refractory prostate carcinoma cell lines by cytokines. *Cancer* **77,** 1862–1872.

[45] Tanabe T, Kominsky SL, Subramaniam PS, Johnson HM, and Torres BA (2000). Inhibition of the glioblastoma cell cycle by type I IFNs occurs at both the G1 and S phases and correlates with the upregulation of p21(WAF1/CIP1). *J Neuro-Oncol* **48,** 225–232.

[46] Street SE, Cretney E, and Smyth MJ (2001). Perforin and interferon-gamma activities independently control tumor initiation, growth, and metastasis. *Blood* **97,** 192–197.

[47] Yan DH, Abramian A, Li Z, Ding Y, Wen Y, Liu TJ, and Hunt K (2003). p202, an interferon-inducible protein, inhibits E2F1-mediated apoptosis in prostate cancer cells. *Biochem Biophys Res Commun* **303,** 219–222.

[48] Wen Y, Yan DH, Wang B, Spohn B, Ding Y, Shao R, Zou Y, Xie K, and Hung MC (2001). p202, an interferon-inducible protein, mediates multiple antitumor activities in human pancreatic cancer xenograft models. *Cancer Res* **61,** 7142–7147.

[49] Feldman AL, Friedl J, Lans TE, Libutti SK, Lorang D, Miller MS, Turner EM, Hewitt SM and Alexander HR (2002). Retroviral gene transfer of interferon-inducible protein 10 inhibits growth of human melanoma xenografts. *Int J Cancer* **99,** 149–153.

[50] Naoe M, Marumoto Y, Ishizaki R, Ogawa Y, Nakagami Y, and Yoshida H (2002). Correlation between major histocompatibility complex class I molecules and $CD8^+$ T lymphocytes in prostate, and quantification of CD8 and interferon-gamma mRNA in prostate tissue specimens. *BJU Int* **90,** 748–753.

[51] Bonham MJ, Galkin A, Montgomery B, Stahl WL, Agus D, and Nelson PS (2002). Effects of the herbal extract PC-SPES on microtubule dynamics and paclitaxel-mediated prostate tumor growth inhibition. *J Natl Cancer Inst* **94,** 1641–1647.

[52] Matejuk A, Dwyer J, Zamora A, Vandenbark AA, and Offner H (2002). Evaluation of the effects of 17beta-estradiol (17beta-e2) on gene expression in experimental autoimmune encephalomyelitis using DNA microarray. *Endocrinology* **143,** 313–319.

[53] Lindner DJ, Kolla V, Kalvakolanu DV, and Borden EC (1997). Tamoxifen enhances interferon-regulated gene expression in breast cancer cells. *Mol Cell Biochem* **167,** 169–177.

[54] Romeo G, Fiorucci G, Chiantore MV, Percario ZA, Vannucchi S, and Affabris E (2002). IRF-1 as a negative regulator of cell proliferation. *J Interferon Cytokine Res* **22,** 39–47.

[55] Bouker KB, Skaar TC, Riggins RB, Harburger DS, Fernandez DR, Zwart A, Wang A, and Clarke R (2005). Interferon regulatory factor-1 (IRF-1) exhibits tumor suppressor activities in breast cancer associated with caspase activation and induction of apoptosis. *Carcinogenesis* **26,** 1527–1535.

[56] Pantel K, Schlimok G, Kutter D, Schaller G, Genz T, Wiebecke B, Backmann R, Funke I, and Riethmuller G (1991). Frequent down-regulation of major histocompatibility class I antigen expression on individual micrometastatic carcinoma cells. *Cancer Res* **51,** 4712–4715.

[57] Cordon-Cardo C, Fuks Z, Drobnjak M, Moreno C, Eisenbach L, and Feldman M (1991). Expression of HLA-A,B,C antigens on primary and metastatic tumor cell populations of human carcinomas. *Cancer Res* **51,** 6372–6380.

[58] Bander NH, Yao D, Liu H, Chen YT, Steiner M, Zuccaro W, and Moy P (1997). MHC class I and II expression in prostate carcinoma and modulation by interferon-alpha and -gamma. *Prostate* **33,** 233–239.

[59] Naoe M, Marumoto Y, Aoki K, Fukagai T, Ogawa Y, Ishizaki R, Nakagami Y, Yoshida H, and Ballo M (2002). MHC-class I expression on prostate carcinoma and modulation by IFN-gamma. *Nippon Hinyokika Gakkai Zasshi* **93,** 532–538.

[60] Lu QL, Abel P, Mitchell S, Foster C, and Lalani EN (2000). Decreased HLA-A expression in prostate cancer is associated with normal allele dosage in the majority of cases. *J Pathol* **190,** 169–176.

[61] Montgomery RB, Bonham M, Nelson PS, Grim J, Makary E, Vessella R, and Stahl WL (2005). Estrogen effects on tubulin expression and taxane mediated cytotoxicity in prostate cancer cells. *Prostate* **65,** 141–150.

[62] Zeng Y, Yokohira M, Saoo K, Takeuchi H, Chen Y, Yamakawa K, Matsuda Y, Kakehi Y, and Imaida K (2005). Inhibition of prostate carcinogenesis in probasin/SV40 T antigen transgenic rats by raloxifene, an antiestrogen with anti-androgen action, but not nimesulide, a selective cyclooxygenase-2 inhibitor. *Carcinogenesis* **26,** 1109–1116.

[63] Shazer RL, Jain A, Galkin AV, Cinman N, Nguyen KN, Natale RB, Gross M, Green L, Bender LI, Holden S, et al. (2006). Raloxifene, an oestrogen-receptor-beta–targeted therapy, inhibits androgen-independent prostate cancer growth: results from preclinical studies and a pilot phase II clinical trial. *BJU Int* **97,** 691–697.

[64] Zhu X, Leav I, Leung YK, Wu M, Liu Q, Gao Y, McNeal JE, and Ho SM (2004). Dynamic regulation of estrogen receptor-beta expression by DNA methylation during prostate cancer development and metastasis. *Am J Pathol* **164,** 2003–2012.

[65] Buttyan R, Zakeri Z, Lockshin R, and Wolgemuth D (1988). Cascade induction of c-fos, c-myc, and heat shock 70K transcripts during regression of the rat ventral prostate gland. *Mol Endocrinol* **2,** 650–657.

[66] Gholz RC, Conde F, and Rutledge DN (2002). Osteoporosis in men treated with androgen suppression therapy for prostate cancer. *Clin J Oncol Nurs* **6,** 88–93.

[67] Cherrier MM (2005). Androgens and cognitive function. *J Endocrinol Invest* **28,** 65–75.